

MorphoSim: An Interactive, Controllable, and Editable Language-guided 4D World Simulator

Xuehai He^{*1}, Shijie Zhou^{*2}, Thivyant Venkateswaran³, Kaizhi Zheng¹,
Ziyu Wan⁴, Achuta Kadambi², Xin Eric Wang¹

¹University of California, Santa Cruz, ²University of California, Los Angeles, ³ IIT Bombay, ⁴ Microsoft
 {xhe89, xwang366}@ucsc.edu

Abstract— World models that support controllable and editable spatiotemporal environments are valuable for robotics, enabling scalable training data, reproducible evaluation, and flexible task design. While recent text-to-video models generate realistic dynamics, they are constrained to 2D views and offer limited interaction. We introduce MorphoSim, a language-guided framework that generates 4D scenes with multi-view consistency and object-level controls. From natural language instructions, MorphoSim produces dynamic environments where objects can be directed, recolored, or removed, and scenes can be observed from arbitrary viewpoints. The framework integrates trajectory-guided generation with feature field distillation, allowing edits to be applied interactively without full re-generation. Experiments show that MorphoSim maintains high scene fidelity while enabling controllability and editability. The code is available at <https://github.com/eric-ai-lab/Morph4D>.

I. INTRODUCTION

Robotics needs world models that support observation from many viewpoints, evolve over time, and accept direct intervention for task specification, data generation, and evaluation. Recent text-to-video models [1], [2], [3], [4], [5] show that large generative models can produce high quality dynamics from language prompts, and there is growing interest in using such models as simulators [6], [7] for robotic environment. Yet most systems remain 2D and single-view, primarily relying on diffusion models or autoregressive models [8], [7], [9], restricting them to single-view observations and non-interactive simulations. These limitations prevent such models from accurately capturing the true complexity of dynamic, multi-view environments. They also do not expose controls that robot learning needs: camera view control, object-level motion control, object insertion or removal, and interactive edit operations.

This paper targets a language-guided 4D (space–time) simulator that supports multi-view rendering and interactive editing at the object level. We ask two questions that are central for robotics: (i) can we lift the capability of visual generation models to 4D (spatial-temporal) scenarios? and (ii) can we expose language-driven controls that change object trajectories and appearance so that

one can script tasks, perturb scenes, and generate diverse training data for visuomotor policies?

We present MorphoSim, a language-guided world simulator that converts natural language commands into editable 4D scenes with consistent multi-view dynamics. By supporting interactive control and object-level editing, MorphoSim enables robotics applications that require flexible scene variation. In particular, it can generate synthetic training data for policy learning, provide controlled perturbations for closed-loop evaluation, and support rapid construction of task variants for studying long-horizon planning. The ability to edit object motion and appearance also facilitates robustness testing of perception systems under viewpoint changes, occlusions, and counterfactual scene modifications. For example, given the instruction “a red cube moves to the plate while the camera circles the table; then make the cube blue and reverse its motion,” MorphoSim produces a temporally coherent, multi-view sequence and applies the specified edits without re-generating the entire scene.

Three challenges arise. First, a suitable embodied scene representation under this situation is not well defined, it must support consistent geometry, appearance, and motion under arbitrary viewpoints. Second, standard text-to-video backbones are optimized for single-view synthesis and do not maintain multi-view coherence or camera control. Third, robotics needs object-level handles (velocity, color, presence) that can be bound to language instructions and edited interactively.

MorphoSim addresses these points with a modular design. A command parameterizer parses language into structured controls for camera and objects; A scene generator produces a 4D representation that supports view-consistent rendering; A scene editor exposes two editing paths: a dynamic control submodule that steers object motion directions and trajectories from language, and a static edit submodule that changes object appearance, extracts objects, or removes them from the scene. The editor operates directly on the 4D representation so that edits are fast and preserve temporal and multi-view consistency.

Our contributions are as follows:

- We present MorphoSim, a new language-guided simulator framework with three components: a *command*

^{*} equal contribution

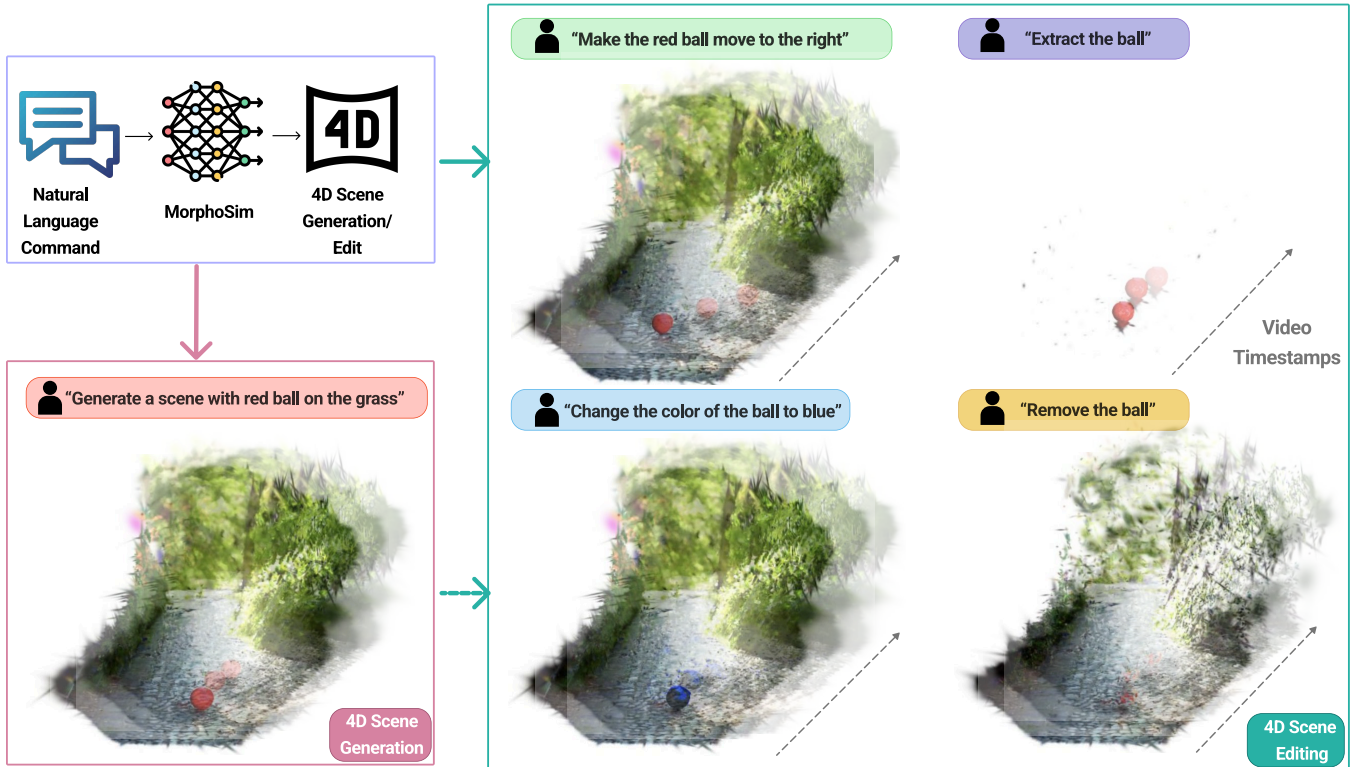


Fig. 1: MorphoSim is a fully natural language-guided 4D scene generation engine that enables generation and editing of 4D scenes based on language commands. Given a natural language input, MorphoSim constructs a 4D scene and provides a unified framework for multiple tasks, including high-quality scene generation, interactive modification of object motion and appearance, and object extraction or removal.

parameterizer, a *scene generator*, and a *scene editor*. Given natural language, it produces view-consistent 4D scenes and supports interactive edits through language.

- The scene editor includes two novel submodule designs: a *Dynamic Control* submodule that changes object motion directions and trajectories from language commands, and a *Static Edit* submodule that changes object appearance (e.g., color), extracts objects, or removes objects.
- We evaluate MorphoSim on robotics-oriented scenarios. Results show high-fidelity 4D scenes and effective control and edit operations that support synthetic data generation and controlled evaluation, with improvements over representative baselines in controllability and editability.

II. RELATED WORKS

Generative Models for 4D Scenes Recent works in diffusion models have revolutionized visual generation across 2D, 3D, and 4D domains. In 2D, frameworks such as Stable Diffusion [10] and Imagen [11] enable high-fidelity text-to-image synthesis and retrieval [12], while cascaded and latent diffusion approaches extend these capabilities to text-to-visual generation [13], [14], [15], [16], [17], [18], [19], [20]. Building upon these successes, diffusion models have transformed visual generation in

3D space [21], [22], [23], [24]. Parallel to these advances, Diffusion priors have further driven 4D scene generation [25], [26], [27], [28], [29], [30], [31], [32], [33], [34], [35], [36], producing realistic spatiotemporal content under constrained settings. Parallel to these advances, efficient scene representations such as 3D Gaussian Splatting (3DGS) [37] have enabled high-fidelity 3D reconstruction and view synthesis, with dynamic extensions [38], [39], [40], [41], [42], [43], [44], [45], [46] modeling temporal deformation fields for 4D consistency. Diffusion priors have further driven 4D scene generation [25], [26], [27], [28], [29], [30], [31], [32], [33], [34], [35], [36], producing realistic spatiotemporal content under constrained settings. For robotics, however, 4D world models must not only render scenes but also support control, editing, and task-driven variation. Our work addresses this gap by introducing a unified, language-guided framework that combines high-quality 4D generation with interactive editing capabilities.

Language-guided Scene Editing Recent advances in language-guided scene editing have shown promising results in static 3D settings by leveraging neural implicit representations and 2D diffusion priors for tasks such as appearance modification [47], [48], [49], [50], [51], [52], [53], [54], object replacement [55], [56], [57], [58], and removal [49], [59], [60]. In the realm of 4D editing, methods like 4D-Editor [61], CTRL-D [62], Control4D [63],

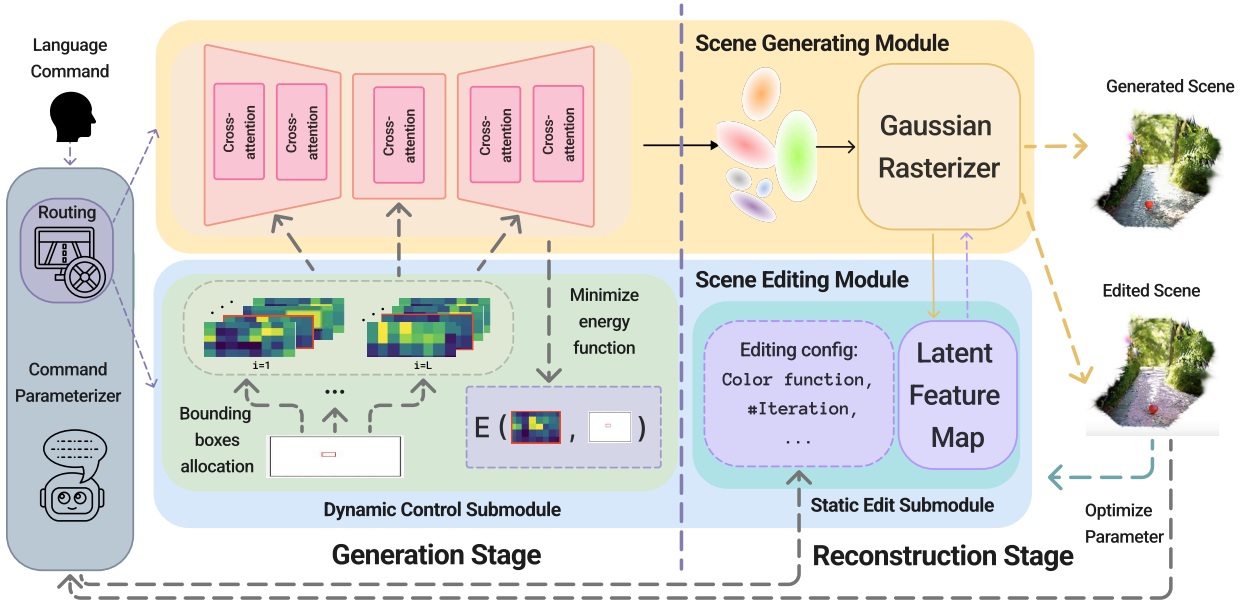


Fig. 2: **Overview of the MorphoSim pipeline.** It consists of a *command parameterizer* for natural language comprehension, a controllable *scene generating module* which supports generation of 4D scenes following dynamic objects motion guidance, and an interactive *scene editing module* for executing edits.

and Instruct 4D-to-4D [64] extend these techniques to dynamic scenes by ensuring temporally consistent appearance edits across frames. Our work advances this line of research by introducing motion control through natural language instructions, thereby enabling not only appearance modifications but also explicit edits to the underlying motion patterns in scenes.

III. MORPHOSIM

MorphoSim is a unified framework that integrates multiple functionalities for generating and editing 4D scenes from natural language input. As illustrated in Figure 2, MorphoSim consists of three core modules: the *Command Parameterizer Module*, the *Scene Generation Module*, and the *Scene Editing Module*. The Command Parameterizer Module serves as the interface between natural language input and system execution. It interprets user instructions, routes them to the appropriate module, and converts them into structured, executable commands. The Scene Generation Module is responsible for generating dynamic scenes based on language descriptions, capturing spatial and temporal instructions. The Scene Editing Module enables interactive modifications, allowing users to adjust motion trajectories, alter object appearances (color), and manipulate scene elements (delete or extract) through natural language instructions. In the following sections, we will introduce these modules in detail.

A. Preliminaries

Video Diffusion Models Video Diffusion Models (VDMs) [13], [65] extend diffusion models to video generation by formulating a fixed forward diffusion process that progressively corrupts a 4D video sample \mathbf{x}_0 with

noise in the latent space. This enables the model to learn a reverse denoising process to recover the original video.

The forward diffusion process consists of T timesteps, where noise is gradually added to the clean data \mathbf{x}_0 through a Markovian parameterization:

$$q(\mathbf{x}_t \mid \mathbf{x}_{t-1}) = \mathcal{N}(\mathbf{x}_t; \sqrt{1 - \beta_t} \mathbf{x}_{t-1}, \beta_t \mathbf{I}), \quad (1)$$

$$q(\mathbf{x}_0 \mid \mathbf{x}_t) = \mathcal{N}(\mathbf{x}_0; \sqrt{\bar{\alpha}_t} \mathbf{x}_t, (1 - \bar{\alpha}_t) \mathbf{I}), \quad (2)$$

where β_t is a predefined variance schedule during diffusion sampling, $\alpha_t = 1 - \beta_t$, and $\bar{\alpha}_t = \prod_{i=1}^t \alpha_i$. The reverse process then attempts to reconstruct \mathbf{x}_{t-1} from \mathbf{x}_t by learning a denoising distribution:

$$p_\theta(\mathbf{x}_{t-1} \mid \mathbf{x}_t) = \mathcal{N}(\mathbf{x}_{t-1}; \boldsymbol{\mu}_\theta(\mathbf{x}_t, t), \boldsymbol{\Sigma}_\theta(\mathbf{x}_t, t)). \quad (3)$$

Here, the mean $\boldsymbol{\mu}_\theta$ and variance $\boldsymbol{\Sigma}_\theta$ are the estimated Gaussian mean and variance predicted by the denoising network. The update step is typically computed as:

$$\mathbf{x}_{t-1} = \frac{1}{\sqrt{\alpha_t}} (\mathbf{x}_t - \sqrt{1 - \alpha_t} \boldsymbol{\mu}_\theta(\mathbf{x}_t, t, \mathbf{c})) + \sigma_t \mathbf{z}, \quad (4)$$

where α_t is the noise schedule coefficient, σ_t is the stochastic noise factor, and $\mathbf{z} \sim \mathcal{N}(0, I)$ represents Gaussian noise injected at each step for improved sample diversity. The latent feature update can be modified to control the generation direction.

3D Gaussian Splatting In dynamic scene reconstruction approaches [43], [44], [46], the scenes were represented with dynamic 3D Gaussians [66]—a set of persistent 3D Gaussians [37] that deform over time to model motion. These representations can efficiently capture spatiotemporal variations in monocular video reconstructions. To create 4D scenes, we build upon MoSca [44],

which reconstruct 4D scenes with single-view partial observations by leveraging priors from 2D foundation models [67], [68], [69], [70], [71] and by imposing regularization constraints on Gaussian motion trajectories. The key in the techniques is the use of 4D Motion Scaffold, a structured graph $(\mathcal{V}, \mathcal{E})$ that governs the deformation of individual 3D Gaussians $\mathcal{G} = \{G_j\}_{j=1}^n$.

B. Language-Guided 4D Scene Generation

1) *LLM as a Command Parameterizer*: Given an input natural language instruction \mathcal{L} , MorphoSim employs a large language model (LLM) agent \mathcal{A} to interpret the command, extract semantic attributes, and dynamically route the request to the appropriate execution module. The agent \mathcal{A} formalizes this routing process by mapping the input \mathcal{L} to an execution plan \mathcal{P} : $\mathcal{A} : \mathcal{L} \rightarrow \mathcal{P} = (\mathcal{M}, \mathcal{Q})$, where $\mathcal{M} \in \{\text{GEN, EDIT}\}$ represents the routing decision, selecting either the scene generating module (\mathcal{G}) or the scene editing module (\mathcal{E}), and \mathcal{Q} represents a set of structured queries extracted from the input.

2) *Scene Generating Module*: If the LLM agent \mathcal{A} determines $\mathcal{M} = \text{GEN}$, it routes the request to the scene generating module \mathcal{G} .

To construct the initial scene representation, we leverage state-of-the-art text-to-video generation models. We introduce an inference-time guidance mechanism that dynamically adjusts motion trajectories while sampling from the conditional distribution: $p(z|y, \mathcal{T}, i)$, where z represents the generated latent features, y is the input text, and \mathcal{T} specifies a predefined trajectory associated with motion-related tokens y_n . This adjustment ensures that generated objects move according to user-specified directions without requiring additional training. The LLM agent first parses the motion direction description from the natural language input into a structured trajectory representation and assigns corresponding bounding boxes. These bounding boxes serve as guidance inputs for the scene generator, ensuring that objects move in the specified direction and at the indicated speed within the generated 4D scene.

Bounding Box Definition. For a given translated trajectory $\mathcal{T} = \{(x_i, y_i, t_i)\}_{i=1}^L$, where L is the number of key points, (x_i, y_i) represents the spatial location at time step t_i , we define the bounding box B_i for frame i as: $B_i = \{(x, y) : |x - x_i| \leq \Delta_x, |y - y_i| \leq \Delta_y\}$, where Δ_x and Δ_y define the spatial tolerance, determining the size of the bounding box. These values are influenced by both object size and the motion attributes extracted from the language.

Frame-Wise Bounding Box Allocation. To account for motion speed and direction, we introduce a velocity-dependent expansion factor. If the language prompt describes fast movement (e.g., "The car moves quickly to the right"), the bounding boxes are spaced farther apart between frames to reflect rapid displacement. We define the displacement vector between consecutive points as: $v_i = \frac{\|(x_{i+1} - x_i, y_{i+1} - y_i)\|}{t_{i+1} - t_i}$, where v_i represents the

velocity magnitude. The bounding box displacement between frames is then scaled by a velocity factor $\lambda(v_i)$: $x_{i+1} = x_i + \lambda v_i \cdot (x_{i+1} - x_i), y_{i+1} = y_i + \lambda v_i \cdot (y_{i+1} - y_i)$. Here, λ is a scaling hyper-parameter that increases with velocity, ensuring that high-speed moving objects specified in the text prompts receive more widely spaced bounding boxes across frames. This adaptive allocation ensures that motion dynamics described in natural language are accurately reflected in the generated scene.

Dynamic Control Submodule. To enforce directional control, we introduce the Dynamic Control Submodule with guidance bounding boxes, where we modify the cross-attention layers by biasing attention scores toward locations along \mathcal{T} . Specifically, at each sampling step i , we adjust the attention response for layers attending to motion-related text tokens. This is implemented using a trajectory-aligned attention weighting mechanism inspired by [72], which directs attention toward spatial regions prescribed by the trajectory. Figure 2 provides an overview of this modification. By dynamically altering attention weight distributions during generation, we effectively steer object placement and movement to align with input descriptions.

Controlling spatial layouts in generative models via cross-attention has been explored in 2D scenarios [73], [18], [74]. We extend this approach by guiding attention maps to follow a predefined trajectory \mathcal{T} over time. The cross-attention score $A_{u,n}$ measures the association between spatial location u and text token y_n , with the sum over tokens constrained to one: $\sum_{n=1}^N A_{u,n} = 1$. To enforce alignment with \mathcal{T} , we bias the attention maps to concentrate within the trajectory-defined bounding boxes B_i at each timestep i . This is achieved through a frame-specific energy function:

$$E_i(A_i, B_i, n) = \left(1 - \frac{\sum_{u \in B_i} A_{i,u,n}}{\sum_u A_{i,u,n}}\right)^2, \quad (5)$$

where $A_{i,u,n}$ represents the attention score at video timestamp i , spatial location u , and text token y_n . Minimizing this energy function encourages the attention distribution to remain within B_i , effectively guiding object placement frame-by-frame. During generation, we iteratively adjust attention maps at each denoising step to minimize E_i and update latent scene features like [72], ensuring that the model remains aligned with \mathcal{T} across successive time steps.

For models adopting the DiT [75] architecture (e.g., [2]), input data is represented as a latent tensor of shape $T \times C \times H \times W$, where T denotes the temporal dimension. The input video data undergoes 3D patchification via a linear projection layer, which extracts non-overlapping patches of size (p_t, p_h, p_w) , where p_t is the patch size for the temporal dimension, p_h is the height, and p_w is the width, and is mapped into token embeddings for the denoiser network. This transforms the latent representation into a sequence of tokens of length $\frac{THW}{p_t p_h p_w}$, ensuring compatibility with the model's spatiotemporal

processing pipeline. To integrate directional guidance into the latent feature updates, we would modify the cross-attention map based on global visual features. Since the input undergoes 3D patch embedding in subsequent processing, we first reshape the latent feature to restore its original spatial-temporal ratio before patchification. This ensures that attention modifications remain spatially coherent and correctly aligned with the scene structure before tokenization.

Scene Reconstruction. Starting from an initial generated scene representation, following [76], [44], we build a dynamic 3D representation that can effectively support the scene editing tasks. Given the monocular representation per frame from the 2D world generator $\mathcal{I} = \{I_1, \dots, I_t\}$, we reconstruct the underlying dynamic 3D scene with a set of dynamic 3D Gaussians, augmented with a unified latent feature embedding that jointly distills various 2D foundation features useful for editing. We leverage dynamic 3D reconstruction to fuse multi-view and multi-frame 2D features into a unified 3D representation.

To achieve this, we augment existing 3D Gaussian attributes with a latent feature \mathcal{F} . We learn \mathcal{F} along with lightweight task-specific decoders $\{\mathcal{D}^1, \dots, \mathcal{D}^S\}$, where the decoder maps the latent feature $\mathcal{F} \in \mathbb{R}^D$ to the editing feature space $\mathcal{F}^s \in \mathbb{R}^{D_s}$.

During optimization, we attach a feature vector $f_j \in \mathbb{R}^D$ to each 3D Gaussian $G_j \in \mathcal{G}$, warp G_j to the target timestep τ following [44], and rasterize f_j using the same approach as Gaussian color c_j in [77]. The RGB and feature reconstruction at viewpoint v and timestep τ are calculated via:

$$\hat{I}_\tau^v = \text{rasterize}(v, \{\text{warp}(G_j, \tau), c_j\}_{G_j \in \mathcal{G}}), \quad (6)$$

$$\hat{F}_\tau^v = \text{rasterize}(v, \{\text{warp}(G_j, \tau), f_j\}_{G_j \in \mathcal{G}}). \quad (7)$$

The reconstructed feature map \hat{F}_τ^v (with viewpoint v omitted for brevity) is passed through the corresponding decoder \mathcal{D}^s to obtain the task-specific feature representation \hat{F}_τ^s , which is supervised against the ground truth feature map obtained from the 2D encoder \mathcal{E}^s . The feature loss L_{feat} is optimized with the original MoScA [44] loss terms:

$$L_{\text{feat}} = \sum_{s=1}^S \text{MSE}(\hat{F}_\tau^s, F_\tau^s), \quad (8)$$

$$\hat{F}_\tau^s = \mathcal{D}^s(\hat{F}_\tau) \quad F_\tau^s = \mathcal{E}^s(I_\tau). \quad (9)$$

Similar to [76], We use an MLP-based decoder trained on 2D rendered feature maps but applied directly to 3D Gaussian features during inference.

C. Scene Editing Module

If the LLM agent \mathcal{A} determines $\mathcal{M} = \text{EDIT}$, it routes the request to the scene editing module \mathcal{E} , which modifies an existing 4D scene \mathcal{S} based on the structured queries \mathcal{Q} . The editing operations include:

- Appearance Editing: Changing the object color.
- Object Manipulation: Removing or extracting objects from the scene.

We further utilize the LLM agent to parse the input languages into executable commands and then perform follow-up executions, such as Color Editing, Object Removal, and Object Extraction. The modules can also be extended to support more executions.

The LLM agent is then used to optimize configuration parameters based on natural language prompts, perform precise queries, and iteratively refine results, enabling intelligent 4D scene manipulation. For instance, given a user instruction such as "Delete the ball" or "Change the ball's color to blue," the agent first parses the prompt and generates a set of configuration options with varying parameters relevant to the task. Specifically, it computes the probability $\mathbf{p}(\tau | j)$ of a 3D Gaussian being associated with a prompt τ : $\mathbf{p}(\tau | j) = \frac{\exp(s)}{\sum_{s_i \in \tau} \exp(s_i)}$, where s is the cosine similarity between the semantic feature f_j of the 3D Gaussian and the query feature $q(\tau)$: $s = \frac{f_j \cdot q(\tau)}{\|f_j\| \|q(\tau)\|}$. The LLM agent then iterates over different threshold values to filter Gaussians with low probability scores and generate sample images using the 4D feature field, evaluating which configuration best aligns with the intended edit.

Once the optimal configuration is determined, the LLM agent \mathcal{A} applies the selected parameters consistently across all frames in the video sequence, ensuring coherence in dynamic 4D scene editing. For instance, when modifying an object's color, the LLM agent iteratively adjusts the threshold to isolate and modify only the target object while preserving the rest of the scene. This process continues until either the input maximum iteration count parameter is reached or the threshold falls below a specified limit, ensuring precise and controlled edits.

IV. EXPERIMENTS

A. Datasets

We evaluate MorphoSim by comparing its generated 4D scenes against real-world videos from the DAVIS dataset [82]. Specifically, we construct textual prompts from DAVIS annotations to generate corresponding 4D scenes and compare with reconstructed 4D scenes from DAVIS videos, assessing their quality relative to real-world counterparts.

B. Quantitative Results on Generated Scene Quality

We evaluate the quality of the reconstructed 4D scenes using four metrics: BRISQUE (Blind/Referenceless Image Spatial Quality Evaluator) [78] is a no-reference image quality assessment metric that measures perceptual distortions based on natural scene statistics; NIQE (Natural Image Quality Evaluator) [79] is another no-reference quality metric that evaluates the deviation of an image from learned natural scene statistics; CLIP Similarity [80] quantifies the semantic consistency between generated

A robotic scorpion crawls from the right to the left



A robotic scorpion crawls from the left to the right



A robotic harvester is moving through the field from left to the right



A robotic harvester is moving through the field from right to the left



Fig. 3: Qualitative examples of 4D scene editing in MorphoSim for object motion control during the generation stage. MorphoSim allows specifying different object motion directions in natural language forms and subsequently changes the scene to ensure objects move according to the given instructions.

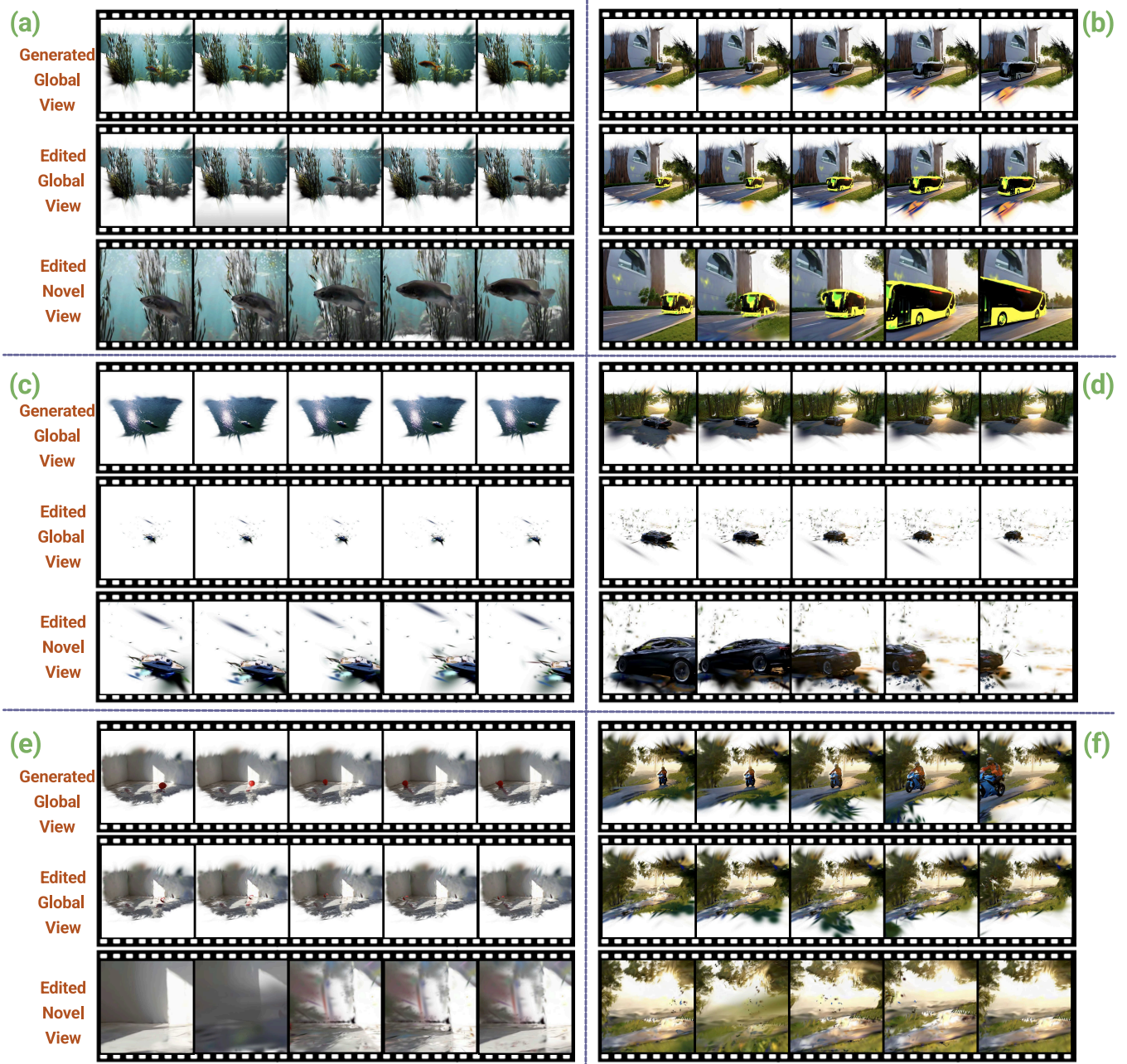


Fig. 4: **Qualitative examples of 4D scene editing in MorphoSim during the reconstruction stage.** (a) and (b) demonstrate *color editing*, (c) and (d) show *object extraction*, while (e) and (f) illustrate *object removal*. In each subfigure: The first row shows the generated global view from the text prompt; The second row presents the global view after scene editing; The third row displays the novel view after editing. The language commands for each example are as follows: (a) "The fish swims through the crystal-clear waters from right to left" to generate the scene, followed by "Make the color of the fish and seaweed black." (b) "The bus is moving from right to left" to generate the scene, followed by "Make the bus yellow." (c) "A serene boat glides gracefully through tranquil waters from left to right" to generate the scene, followed by "Extract the boat." (d) "A car is moving from right to left through a serene sunlit landscape" to generate the scene, followed by "Extract the car." (e) "A small, vibrant red rubber ball is bouncing from right to left" to generate the scene, followed by "Delete the ball." (f) "A sleek black motorcycle is gliding effortlessly from right to left" to generate the scene, followed by "Delete the motorcycle."

and real-world scenes by computing the cosine similarity between image embeddings extracted from the CLIP

model; QAlign [81] is the current state-of-the-art method for image quality assessment, leveraging a large mul-

TABLE I: Quantitative comparison between real-world scenes (Davis) and MorphoSim generated 4D scenes with two different base models.

Method	BRISQUE [78] ↓	NIQE [79] ↓	CLIP Similarity [80] ↑	QAlign Quality [81] ↑	QAlign Aesthetic [81] ↑
<i>Overall Average</i>					
Davis (Real)	31.639	3.551	0.250	3.432	2.254
Backbone I	18.380	3.286	0.263	3.350	2.114
Backbone II	23.411	3.392	0.261	3.309	2.074
<i>Example Scene Comparisons:</i>					
<i>Scene: sheep</i>					
Davis (Real)	18.090	2.173	0.266	4.371	2.891
Backbone I	9.638	3.454	0.300	3.623	1.918
Backbone II	14.476	3.951	0.290	3.734	2.071
<i>Scene: snowboard</i>					
Davis (Real)	34.904	3.719	0.269	2.715	1.991
Backbone I	18.163	2.836	0.313	4.011	2.306
Backbone II	29.504	3.412	0.279	2.451	1.970
<i>Scene: elephant</i>					
Davis (Real)	16.815	2.317	0.284	4.048	2.764
Backbone I	15.140	3.171	0.308	3.634	2.511
Backbone II	16.877	3.982	0.301	3.765	2.590

timodal model fine-tuned on publicly available image quality assessment datasets.

The results are summarized in Table I, where we compare our method on two video generation backbones with real-world scenes (Davis). Backbone I is modified from CogVideoX [83], and Backbone II is modified from Cosmos [2] to achieve spatial control and 4D scene generation. The results demonstrate that our generated 4D scenes achieve comparable or better quality than real-world scenes using both two backbones, with Backbone I showing significantly better BRISQUE scores, slightly better NIQE scores, and improved CLIP similarity. This improvement can be attributed to the quality of MorphoSim generated 4D scenes, as well as the fact that MorphoSim generated camera views remain fixed throughout, resulting in higher metric scores, whereas real-world video sequences typically involve dynamic camera movement, which can introduce additional variance in evaluation.

C. Qualitative Results

We present qualitative results demonstrating the capabilities of our method in 4D scene generation and editing. As shown in Figure 4, our approach generates 4D scenes with realism comparable to real-world environments. Additionally, it enables dynamic object motion editing, allowing objects to be manipulated to move in different directions based on user instructions (Figure 3). Beyond motion control, our method supports appearance modifications, such as color editing (Figure 4), ensuring consistent alterations across frames. Moreover, it facilitates structural modifications, including object extraction, which isolates objects without disrupting the surrounding scene, and object removal, which eliminates target objects while preserving background coherence. These results highlight the versatility of our approach in controlling, modifying, and refining 4D scene generation.

V. CONCLUSION

We introduced MorphoSim, a framework for language-guided generation and interactive editing of 4D scenes. By combining large language models with trajectory-guided generation and feature field distillation, MorphoSim produces dynamic, view-consistent environments that can be modified at the object level through natural language commands. We believe that such simulation tools can accelerate progress in robot learning and provide a flexible platform for perception, planning, and interaction.

REFERENCES

- [1] KlingAI. Kling. <https://kling.kuaishou.com/en>. (Accessed on 09/22/2024).
- [2] NVIDIA, ;, Niket Agarwal, Arslan Ali, Maciej Bala, Yogesh Balaji, Erik Barker, Tiffany Cai, Prithvijit Chattopadhyay, Yongxin Chen, Yin Cui, Yifan Ding, Daniel Dworakowski, Jiaoqiao Fan, Michele Fenzi, Francesco Ferroni, Sanja Fidler, Dieter Fox, Songwei Ge, Yunhao Ge, Jinwei Gu, Siddharth Gururani, Ethan He, Jiahui Huang, Jacob Huffman, Pooya Jannaty, Jingyi Jin, Seung Wook Kim, Gergely Klár, Grace Lam, Shiyi Lan, Laura Leal-Taixe, Anqi Li, Zhaoshuo Li, Chen-Hsuan Lin, Tsung-Yi Lin, Huan Ling, Ming-Yu Liu, Xian Liu, Alice Luo, Qianli Ma, Hanzi Mao, Kaichun Mo, Arsalan Mousavian, Seungjun Nah, Sriharsha Niverty, David Page, Despoina Paschalidou, Zeeshan Patel, Lindsey Pavao, Morteza Ramezanali, Fitsum Reda, Xiaowei Ren, Vasanth Rao Naik Sabavat, Ed Schmerling, Stella Shi, Bartosz Stefański, Shitao Tang, Lyne Tchapmi, Przemek Tredak, Wei-Cheng Tseng, Jibin Varghese, Hao Wang, Haoxiang Wang, Heng Wang, Ting-Chun Wang, Fangyin Wei, Xinyue Wei, Jay Zhangjie Wu, Jiashu Xu, Wei Yang, Lin Yen-Chen, Xiaohui Zeng, Yu Zeng, Jing Zhang, Qinsheng Zhang, Yuxuan Zhang, Qingqing Zhao, and Artur Zolkowski. Cosmos world foundation model platform for physical ai. *arXiv preprint arXiv: 2501.03575*, 2025.
- [3] Haoxin Chen, Yong Zhang, Xiaodong Cun, Menghan Xia, Xintao Wang, Chao Weng, and Ying Shan. Videocrafter2: Overcoming data limitations for high-quality video diffusion models, 2024.
- [4] Wan Team. Wan: Open and advanced large-scale video generative models. 2025.
- [5] Hunyuan team. Hunyuanvideo: A systematic framework for large video generative models, 2024.

[6] Bingyi Kang, Yang Yue, Rui Lu, Zhiping Lin, Yang Zhao, Kaixin Wang, Gao Huang, and Jiashi Feng. How far is video generation from world model: A physical law perspective. *arXiv preprint arXiv:2411.02385*, 2024.

[7] Xiaofeng Wang, Zheng Zhu, Guan Huang, Boyuan Wang, Xinze Chen, and Jiwen Lu. Worlddreamer: Towards general world models for video generation via predicting masked tokens. *arXiv preprint arXiv:2401.09985*, 2024.

[8] Jiannan Xiang, Guangyi Liu, Yi Gu, Qiyue Gao, Yuting Ning, Yuheng Zha, Zeyu Feng, Tianhua Tao, Shibo Hao, Yemin Shi, Zhengzhong Liu, Eric P. Xing, and Zhiting Hu. Pandora: Towards general world model with natural language actions and video states. 2024.

[9] Keyu Tian, Yi Jiang, Zehuan Yuan, Bingyue Peng, and Liwei Wang. Visual autoregressive modeling: Scalable image generation via next-scale prediction. *Neural Information Processing Systems*, 2024.

[10] Robin Rombach, Andreas Blattmann, Dominik Lorenz, Patrick Esser, and Björn Ommer. High-resolution image synthesis with latent diffusion models. In *Proceedings of the IEEE/CVF Conference on Computer Vision and Pattern Recognition*, pages 10684–10695, 2022.

[11] Chitwan Saharia, William Chan, Saurabh Saxena, Lala Li, Jay Whang, Emily Denton, Seyed Kamyar Seyed Ghasemipour, Burcu Karagol Ayan, S. Sara Mahdavi, Rapha Gontijo Lopes, Tim Salimans, Jonathan Ho, David J Fleet, and Mohammad Norouzi. Photorealistic text-to-image diffusion models with deep language understanding. *arXiv:2205.11487*, 2022.

[12] Xuehai He, Weixi Feng, Tsu-Jui Fu, Varun Jampani, Arjun Akula, Pradyumna Narayana, Sugato Basu, William Yang Wang, and Xin Eric Wang. Discffusion: Discriminative diffusion models as few-shot vision and language learners. *arXiv preprint arXiv:2305.10722*, 2023.

[13] Yingqing He, Tianyu Yang, Yong Zhang, Ying Shan, and Qifeng Chen. Latent video diffusion models for high-fidelity long video generation. *arXiv preprint arXiv:2211.13221*, 2022.

[14] Jiaqi Xu, Xinyi Zou, Kunzhe Huang, Yunkuo Chen, Bo Liu, MengLi Cheng, Xing Shi, and Jun Huang. Eeasyanimate: A high-performance long video generation method based on transformer architecture. *arXiv preprint arXiv:2405.18991*, 2024.

[15] Zangwei Zheng, Xiangyu Peng, Tianji Yang, Chenhui Shen, Shenggui Li, Hongxin Liu, Yukun Zhou, Tianyi Li, and Yang You. Open-sora: Democratizing efficient video production for all, March 2024.

[16] Xuehai He, Jian Zheng, Jacob Zhiyuan Fang, Robinson Piramuthu, Mohit Bansal, Vicente Ordóñez, Gunnar A Sigurdsson, Nanyun Peng, and Xin Eric Wang. Flexecontrol: Flexible and efficient multimodal control for text-to-image generation. *arXiv preprint arXiv:2405.04834*, 2024.

[17] PKU-Yuan Lab and Tuzhan AI etc. Open-sora-plan, April 2024.

[18] Weixi Feng, Xuehai He, Tsu-Jui Fu, Varun Jampani, Arjun Akula, Pradyumna Narayana, Sugato Basu, Xin Eric Wang, and William Yang Wang. Training-free structured diffusion guidance for compositional text-to-image synthesis. *arXiv preprint arXiv:2212.05032*, 2022.

[19] Zhuoyi Yang, Jiayan Teng, Wendi Zheng, Ming Ding, Shiyu Huang, Jiazheng Xu, Yuanming Yang, Wenyi Hong, Xiaohan Zhang, Guanyu Feng, et al. Cogvideox: Text-to-video diffusion models with an expert transformer. *arXiv preprint arXiv:2408.06072*, 2024.

[20] Vchitect. Vchitect 2.0. <https://github.com/Vchitect/Vchitect-2.0>, 2024. Version 2.0, Accessed: 2024-11-09.

[21] Fangfu Liu, Diankun Wu, Yi Wei, Yongming Rao, and Yueqi Duan. Sherpa3d: Boosting high-fidelity text-to-3d generation via coarse 3d prior. In *Proceedings of the IEEE/CVF Conference on Computer Vision and Pattern Recognition*, pages 20763–20774, 2024.

[22] Weixi Feng, Wanrong Zhu, Tsu-jui Fu, Varun Jampani, Arjun Akula, Xuehai He, Sugato Basu, Xin Eric Wang, and William Yang Wang. Layoutgpt: Compositional visual planning and generation with large language models. *Advances in Neural Information Processing Systems*, 36:18225–18250, 2023.

[23] Zhaoxi Chen, Jiaxiang Tang, Yuhao Dong, Ziang Cao, Fangzhou Hong, Yushi Lan, Tengfei Wang, Haozhe Xie, Tong Wu, Shunsuke Saito, et al. 3dtopia-xl: Scaling high-quality 3d asset generation via primitive diffusion. *arXiv preprint arXiv:2409.12957*, 2024.

[24] Shuang Wu, Youtian Lin, Feihu Zhang, Yifei Zeng, Jingxi Xu, Philip Torr, Xun Cao, and Yao Yao. Direct3d: Scalable image-to-3d generation via 3d latent diffusion transformer. *arXiv preprint arXiv:2405.14832*, 2024.

[25] Uriel Singer, Shelly Sheynin, Adam Polyak, Oron Ashual, Iurii Makarov, Filippos Kokkinos, Naman Goyal, Andrea Vedaldi, Devi Parikh, Justin Johnson, et al. Text-to-4d dynamic scene generation. *arXiv preprint arXiv:2301.11280*, 2023.

[26] Heng Yu, Chaoyang Wang, Peiye Zhuang, Willi Menapace, Aliaksandr Siarohin, Junli Cao, László Jeni, Sergey Tulyakov, and Hsin-Ying Lee. 4real: Towards photorealistic 4d scene generation via video diffusion models. *Advances in Neural Information Processing Systems*, 37:45256–45280, 2025.

[27] Sherwin Bahmani, Xian Liu, Wang Yifan, Ivan Skorokhodov, Victor Rong, Ziwei Liu, Xihui Liu, Jeong Joon Park, Sergey Tulyakov, Gordon Wetzstein, et al. Tc4d: Trajectory-conditioned text-to-4d generation. In *European Conference on Computer Vision*, pages 53–72. Springer, 2024.

[28] Yuyang Zhao, Zhiwen Yan, Enze Xie, Lanqing Hong, Zhenguo Li, and Gim Hee Lee. Animate124: Animating one image to 4d dynamic scene. *arXiv preprint arXiv:2311.14603*, 2023.

[29] Sherwin Bahmani, Ivan Skorokhodov, Victor Rong, Gordon Wetzstein, Leonidas Guibas, Peter Wonka, Sergey Tulyakov, Jeong Joon Park, Andrea Tagliasacchi, and David B Lindell. 4d-fy: Text-to-4d generation using hybrid score distillation sampling. In *Proceedings of the IEEE/CVF Conference on Computer Vision and Pattern Recognition*, pages 7996–8006, 2024.

[30] Huan Ling, Seung Wook Kim, Antonio Torralba, Sanja Fidler, and Karsten Kreis. Align your gaussians: Text-to-4d with dynamic 3d gaussians and composed diffusion models. In *Proceedings of the IEEE/CVF conference on computer vision and pattern recognition*, pages 8576–8588, 2024.

[31] Jiawei Ren, Liang Pan, Jiaxiang Tang, Chi Zhang, Ang Cao, Gang Zeng, and Ziwei Liu. Dreamgaussian4d: Generative 4d gaussian splatting. *arXiv preprint arXiv:2312.17142*, 2023.

[32] Dejia Xu, Hanwen Liang, Neel P Bhatt, Hezhen Hu, Hanxue Liang, Konstantinos N Plataniotis, and Zhangyang Wang. Comp4d: Llm-guided compositional 4d scene generation. *arXiv preprint arXiv:2403.16993*, 2024.

[33] Yuyang Yin, Dejia Xu, Zhangyang Wang, Yao Zhao, and Yunchao Wei. 4dgen: Grounded 4d content generation with spatial-temporal consistency. *arXiv preprint arXiv:2312.17225*, 2023.

[34] Jiawei Ren, Kevin Xie, Ashkan Mirzaei, Hanxue Liang, Xiaohui Zeng, Karsten Kreis, Ziwei Liu, Antonio Torralba, Sanja Fidler, Seung Wook Kim, et al. L4gm: Large 4d gaussian reconstruction model. *arXiv preprint arXiv:2406.10324*, 2024.

[35] Renjie Li, Panwang Pan, Bangbang Yang, Dejia Xu, Shijie Zhou, Xuanyang Zhang, Zeming Li, Achuta Kadambi, Zhangyang Wang, and Zhiwen Fan. 4k4dgen: Panoramic 4d generation at 4k resolution. *arXiv preprint arXiv:2406.13527*, 2024.

[36] Qi Sun, Zhiyang Guo, Ziyu Wan, Jing Nathan Yan, Shengming Yin, Wengang Zhou, Jing Liao, and Houqiang Li. Eg4d: Explicit generation of 4d object without score distillation. *arXiv preprint arXiv:2405.18132*, 2024.

[37] Bernhard Kerbl, Georgios Kopanas, Thomas Leimkühler, and George Drettakis. 3d gaussian splatting for real-time radiance field rendering. *ACM Transactions on Graphics (ToG)*, 42(4):1–14, 2023.

[38] Guanjun Wu, Taoran Yi, Jiemin Fang, Lingxi Xie, Xiaopeng Zhang, Wei Wei, Wenyu Liu, Qi Tian, and Xinggang Wang. 4d gaussian splatting for real-time dynamic scene rendering. *arXiv preprint arXiv:2310.08528*, 2023.

[39] Yuanxing Duan, Fangyin Wei, Qiyu Dai, Yuhang He, Wenzheng Chen, and Baoquan Chen. 4d gaussian splatting: Towards efficient novel view synthesis for dynamic scenes. *arXiv preprint arXiv:2402.03307*, 2024.

[40] Zeyu Yang, Hongye Yang, Zijie Pan, Xiatian Zhu, and Li Zhang. Real-time photorealistic dynamic scene representation and rendering with 4d gaussian splatting. *arXiv preprint arXiv:2310.10642*, 2023.

[41] Yi-Hua Huang, Yang-Tian Sun, Ziyi Yang, Xiaoyang Lyu, Yan-Pei Cao, and Xiaojuan Qi. Sc-gs: Sparse-controlled gaussian splatting for editable dynamic scenes. In *Proceedings of the IEEE/CVF Conference on Computer Vision and Pattern Recognition*, pages 4220–4230, 2024.

[42] Yiqing Liang, Numair Khan, Zhengqin Li, Thu Nguyen-Phuoc, Douglas Lanman, James Tompkin, and Lei Xiao. Gaufre: Gaussian deformation fields for real-time dynamic novel view synthesis. *arXiv preprint arXiv:2312.11458*, 2023.

[43] Qianqian Wang, Vickie Ye, Hang Gao, Jake Austin, Zhengqi Li, and Angjoo Kanazawa. Shape of motion: 4d reconstruction from a single video. *arXiv preprint arXiv:2407.13764*, 2024.

[44] Jiahui Lei, Yijia Weng, Adam Harley, Leonidas Guibas, and Kostas Daniilidis. Mosca: Dynamic gaussian fusion from casual videos via 4d motion scaffolds. *arXiv preprint arXiv:2405.17421*, 2024.

[45] Marko Mihajlovic, Sergey Prokudin, Siyu Tang, Robert Maier, Federica Bogo, Tony Tung, and Edmond Boyer. Splatfields: Neural gaussian splats for sparse 3d and 4d reconstruction. In *European Conference on Computer Vision*, pages 313–332. Springer, 2025.

[46] Colton Stearns, Adam Harley, Mikaela Uy, Florian Dubost, Federico Tombari, Gordon Wetzstein, and Leonidas Guibas. Dynamic gaussian marbles for novel view synthesis of casual monocular videos. *arXiv preprint arXiv:2406.18717*, 2024.

[47] Yiwen Chen, Zilong Chen, Chi Zhang, Feng Wang, Xiaofeng Yang, Yikai Wang, Zhongang Cai, Lei Yang, Huaping Liu, and Guosheng Lin. Gaussianeditor: Swift and controllable 3d editing with gaussian splatting. In *Proceedings of the IEEE/CVF conference on computer vision and pattern recognition*, pages 21476–21485, 2024.

[48] Junjie Wang, Jiemin Fang, Xiaopeng Zhang, Lingxi Xie, and Qi Tian. Gaussianeditor: Editing 3d gaussians delicately with text instructions. In *Proceedings of the IEEE/CVF conference on computer vision and pattern recognition*, pages 20902–20911, 2024.

[49] Jingyu Zhuang, Chen Wang, Liang Lin, Lingjie Liu, and Guanbin Li. Dreameditor: Text-driven 3d scene editing with neural fields. In *SIGGRAPH Asia 2023 Conference Papers*, pages 1–10, 2023.

[50] Umar Khalid, Hasan Iqbal, Nazmul Karim, Muhammad Tayyab, Jing Hua, and Chen Chen. Latenteditor: text driven local editing of 3d scenes. In *European Conference on Computer Vision*, pages 364–380. Springer, 2024.

[51] Etai Sella, Gal Fiebelman, Peter Hedman, and Hadar Averbuch-Elor. Vox-e: Text-guided voxel editing of 3d objects. *arXiv preprint arXiv:2303.12048*, 2023.

[52] Yunqiu Xu, Linchao Zhu, and Yi Yang. Gg-editor: Locally editing 3d avatars with multimodal large language model guidance. In *Proceedings of the 32nd ACM International Conference on Multimedia*, pages 10910–10919, 2024.

[53] Shuangkang Fang, Yufeng Wang, Yi-Hsuan Tsai, Yi Yang, Wenrui Ding, Shuchang Zhou, and Ming-Hsuan Yang. Chat-edit-3d: Interactive 3d scene editing via text prompts. In *European Conference on Computer Vision*, pages 199–216. Springer, 2024.

[54] Jing Wu, Jia-Wang Bian, Xinghui Li, Guangrun Wang, Ian Reid, Philip Torr, and Victor Adrian Prisacariu. Gaussctrl: Multi-view consistent text-driven 3d gaussian splatting editing. In *European Conference on Computer Vision*, pages 55–71. Springer, 2024.

[55] Edward Bartrum, Thu Nguyen-Phuoc, Chris Xie, Zhengqin Li, Numair Khan, Armen Avetisyan, Douglas Lanman, and Lei Xiao. Replaceanything3d: Text-guided 3d scene editing with compositional neural radiance fields. *arXiv preprint arXiv:2401.17895*, 2024.

[56] Kaizhi Zheng, Xiaotong Chen, Xuehai He, Jing Gu, Linjie Li, Zhengyuan Yang, Kevin Lin, Jianfeng Wang, Lijuan Wang, and Xin Eric Wang. Editroom: LLM-parameterized graph diffusion for composable 3d room layout editing. In *The Thirteenth International Conference on Learning Representations*, 2025.

[57] Jingyu Zhuang, Di Kang, Yan-Pei Cao, Guanbin Li, Liang Lin, and Ying Shan. Tip-editor: An accurate 3d editor following both text-prompts and image-prompts. *ACM Transactions on Graphics (TOG)*, 43(4):1–12, 2024.

[58] Ori Gordon, Omri Avrahami, and Dani Lischinski. Blended-nerf: Zero-shot object generation and blending in existing neural radiance fields. In *Proceedings of the IEEE/CVF International Conference on Computer Vision*, pages 2941–2951, 2023.

[59] Mingqiao Ye, Martin Danelljan, Fisher Yu, and Lei Ke. Gaussian grouping: Segment and edit anything in 3d scenes. In *ECCV*, 2024.

[60] Ri-Zhao Qiu, Ge Yang, Weijia Zeng, and Xiaolong Wang. Feature splatting: Language-driven physics-based scene synthesis and editing. *arXiv preprint arXiv:2404.01223*, 2024.

[61] Dadong Jiang, Zhihui Ke, Xiaobo Zhou, and Xidong Shi. 4d-editor: Interactive object-level editing in dynamic neural radiance fields via semantic distillation. *arXiv preprint arXiv:2310.16858*, 2023.

[62] Kai He, Chin-Hsuan Wu, and Igor Gilitschenski. Ctrl-d: Controllable dynamic 3d scene editing with personalized 2d diffusion. *arXiv preprint arXiv:2412.01792*, 2024.

[63] Ruizhi Shao, Jingxiang Sun, Cheng Peng, Zerong Zheng, Boyao Zhou, Hongwen Zhang, and Yebin Liu. Control4d: Efficient 4d portrait editing with text. In *Proceedings of the IEEE/CVF Conference on Computer Vision and Pattern Recognition*, pages 4556–4567, 2024.

[64] Linzhan Mou, Jun-Kun Chen, and Yu-Xiong Wang. Instruct 4d-to-4d: Editing 4d scenes as pseudo-3d scenes using 2d diffusion. In *Proceedings of the IEEE/CVF Conference on Computer Vision and Pattern Recognition*, pages 20176–20185, 2024.

[65] Andreas Blattmann, Tim Dockhorn, Sumith Kulal, Daniel Mendelevitch, Maciej Kilian, Dominik Lorenz, Yam Levi, Zion English, Vikram Voleti, Adam Letts, Varun Jampani, and Robin Rombach. Stable video diffusion: Scaling latent video diffusion models to large datasets. *NONE*, 2023.

[66] Jonathon Luiten, Georgios Kopanas, Bastian Leibe, and Deva Ramanan. Dynamic 3d gaussians: Tracking by persistent dynamic view synthesis. *arXiv preprint arXiv:2308.09713*, 2023.

[67] Luigi Piccinelli, Yung-Hsu Yang, Christos Sakaridis, Mattia Segu, Siyu Li, Luc Van Gool, and Fisher Yu. Unidepth: Universal monocular metric depth estimation. *arXiv preprint arXiv:2403.18913*, 2024.

[68] Shariq Farooq Bhat, Reiner Birk, Diana Wofk, Peter Wonka, and Matthias Müller. Zoodepth: Zero-shot transfer by combining relative and metric depth. *arXiv preprint arXiv:2302.12288*, 2023.

[69] Zachary Teed and Jia Deng. Raft: Recurrent all-pairs field transforms for optical flow. In *ECCV*, 2020.

[70] Nikita Karaev, Ignacio Rocco, Benjamin Graham, Natalia Neverova, Andrea Vedaldi, and Christian Rupprecht. Cotracker: It is better to track together. *arXiv preprint arXiv:2307.07635*, 2023.

[71] Adam W Harley, Zhaoyuan Fang, and Katerina Fragkiadaki. Particle video revisited: Tracking through occlusions using point trajectories. In *European Conference on Computer Vision*, pages 59–75. Springer, 2022.

[72] Xuehai He, Shuohang Wang, Jianwei Yang, Xiaoxia Wu, Yiping Wang, Kuan Wang, Zheng Zhan, Olatunji Ruwase, Yelong Shen, and Xin Eric Wang. Mojito: Motion trajectory and intensity control for video generation. *arXiv preprint arXiv: 2412.08948*, 2024.

[73] Amir Hertz, Ron Mokady, Jay Tenenbaum, Kfir Aberman, Yael Pritch, and Daniel Cohen-Or. Prompt-to-prompt image editing with cross attention control. *arXiv preprint arXiv:2208.01626*, 2022.

[74] Minghao Chen, Iro Laina, and Andrea Vedaldi. Training-free layout control with cross-attention guidance. In *Proceedings of the IEEE/CVF Winter Conference on Applications of Computer Vision*, pages 5343–5353, 2024.

[75] William S. Peebles and Saining Xie. Scalable diffusion models with transformers. *IEEE International Conference on Computer Vision*, 2022.

- [76] Shijie Zhou, Hui Ren, Yijia Weng, Shuwang Zhang, Zhen Wang, Dejia Xu, Zhiwen Fan, Suya You, Zhangyang Wang, Leonidas Guibas, et al. Feature4x: Bridging any monocular video to 4d agentic ai with versatile gaussian feature fields. In *Proceedings of the Computer Vision and Pattern Recognition Conference*, pages 14179–14190, 2025.
- [77] Shijie Zhou, Haoran Chang, Sicheng Jiang, Zhiwen Fan, Zehao Zhu, Dejia Xu, Pradyumna Chari, Suya You, Zhangyang Wang, and Achuta Kadambi. Feature 3dgs: Supercharging 3d gaussian splatting to enable distilled feature fields. In *Proceedings of the IEEE/CVF Conference on Computer Vision and Pattern Recognition*, pages 21676–21685, 2024.
- [78] Anish Mittal, Anush Krishna Moorthy, and Alan Conrad Bovik. No-reference image quality assessment in the spatial domain. *IEEE Transactions on image processing*, 21(12):4695–4708, 2012.
- [79] Anish Mittal, Anush Krishna Moorthy, and Alan Conrad Bovik. No-reference image quality assessment in the spatial domain. *IEEE Transactions on image processing*, 21(12):4695–4708, 2012.
- [80] Alec Radford, Jong Wook Kim, Chris Hallacy, Aditya Ramesh, Gabriel Goh, Sandhini Agarwal, Girish Sastry, Amanda Askell, Pamela Mishkin, Jack Clark, et al. Learning transferable visual models from natural language supervision. *arXiv preprint arXiv:2103.00020*, 2021.
- [81] Haoning Wu, Zicheng Zhang, Weixia Zhang, Chaofeng Chen, Liang Liao, Chunyi Li, Yixuan Gao, Annan Wang, Erli Zhang, Wenxiu Sun, Qiong Yan, Xiongkuo Min, Guangtao Zhai, and Weisi Lin. Q-align: Teaching lmms for visual scoring via discrete text-defined levels. *International Conference on Machine Learning*, 2023.
- [82] Jordi Pont-Tuset, Federico Perazzi, Sergi Caelles, Pablo Arbeláez, Alex Sorkine-Hornung, and Luc Van Gool. The 2017 davis challenge on video object segmentation. *arXiv preprint arXiv:1704.00675*, 2017.
- [83] Wenyi Hong, Ming Ding, Wendi Zheng, Xinghan Liu, and Jie Tang. Cogvideo: Large-scale pretraining for text-to-video generation via transformers. *arXiv preprint arXiv:2205.15868*, 2022.